Supporting Information:

Unveiling the Far Infrared – to – Ultraviolet Optical Properties of Bismuth for Applications in Plasmonics and Nanophotonics

Johann Toudert[1,*,+], Rosalia Serna[1,#], Iván Camps[1], Jacek Wojcik[2], Peter Mascher[2], Esther Rebollar[3], Tiberio A. Ezquerra[4]

[1]Laser Processing Group (LPG), Instituto de Óptica, CSIC, Madrid, Spain
*mail to: johann.toudert@gmail.com
[+]present address: ICFO-Institut de Ciencies Fotoniques, The Barcelona Institute of Science and Technology, 08860 Castelldefels (Barcelona), Spain
[#]mail to: rosalia.serna@csic.es
[2]Department of Engineering Physics and Centre for Emerging Device Technologies, McMaster University, Hamilton, Ontario, Canada
[3]Instituto de Química Física Rocasolano, IQFR-CSIC, Madrid, Spain
[4]Instituto de Estructura de la Materia (IEM), CSIC, Madrid, Spain

S1. Parameters of the Drude Function and Lorentz Oscillators and Parameter Correlation

The dielectric function $\varepsilon = \varepsilon_1 + j\varepsilon_2$ of the dense Bi layer was described as the sum of a Drude function and 9 Kramers Kronig – consistent Lorentz oscillators:

$$\varepsilon = \varepsilon_{Drude} + \Sigma_{(i=1\ to\ 9)}\ \varepsilon_{Lorentz,i}$$

The Drude function was written as (Drude N-µ (0) function of the WVASE32 software):

$$\varepsilon_{Drude} = -[he^2N/(2\pi\varepsilon_0 m)]\tau/(\tau E^2 + jhE/2\pi)$$

With N the density of free carriers, m the effective mass of the free carriers, E the photon energy and τ the collision time; the best fit was obtained with $N = 1.85.10^{18}$ cm^{-3}, m* = m/mass of the electron = 0.01 and τ = 29 fs.

The Lorentz oscillators were written as (Lor (0, eV) function of the WVASE32 software):

$$\varepsilon_{Lorentz,i} = A_i Br_i E_i/(E_i^2 - E^2 - jBr_i E)$$

Where A_i is related with the amplitude of the ith oscillator; Br_i being its damping factor and E_i driving its peak energy. The best fit was obtained for the Lorentz oscillator parameters given in **table S1** below.

i	A_i (dimensionless)	E_i (eV)	Br_i (eV)
1	38.085	0.77397	0.40956
2	22.508	1.5037	1.0772
3	194.33	31.137	0.4074
4	55.445	0.98272	0.7065
5	3.2131	2.5971	0.78196
6	2.794	5.1145	1.8165
7	0.89563	3.00	0.35318
8	29.502	0.6476	0.45805
9	9.2321	0.12654	0.20

Table S1. Best fit parameters of the Lorentz oscillators.

In view of the large number of parameters involved in the ellipsometry data analysis (parameters of 9 oscillators, of the Drude function, and the film and roughness layer thicknesses), it is worth discussing their correlation. This can be done from the correlation matrix associated with the best fit, shown below.

	rho	tau	A_1	E_1	Br_1	A_2	E_2	Br_2	A_3	E_3	Br_3	A_4	E_4	Br_4	A_5	E_5	Br_5	A_6	E_6	Br_6	A_7	E_7	Br_7	A_8	E_8	Br_8	A_9	E_9	Br_9	t_{Bi}	t_{rough}
t_{rough}	-0.2	0.1	0.2	0.0	0.2	0.2	-0.1	0.1	0.2	-0.2	-0.2	-0.2	0.2	-0.1	0.3	0.0	0.0	0.2	0.1	0.1	0.1	0.0	0.0	-0.1	0.0	0.2	0.1	0.0	0.1	-0.7	1.0
t_{Bi}	0.2	-0.1	-0.3	0.1	-0.3	-0.2	0.1	-0.1	-0.1	0.0	0.1	0.2	-0.2	0.1	-0.2	0.0	0.0	-0.1	-0.1	-0.1	0.0	0.0	0.3	0.2	-0.1	-0.2	0.0	0.0	-0.1	1.0	-0.7
Br_9	-0.6	0.7	0.5	0.1	0.5	0.4	-0.4	0.4	-0.3	0.3	0.3	-0.5	0.5	-0.4	0.1	0.0	0.0	-0.2	-0.1	-0.2	0.1	0.0	0.1	-0.3	-0.3	0.1	0.4	0.8	1.0	-0.1	0.1
E_9	-0.1	0.2	0.6	0.1	0.5	0.5	-0.5	0.5	-0.4	0.4	0.4	-0.6	0.6	-0.5	0.1	0.0	0.0	-0.3	-0.2	-0.2	0.1	0.0	0.1	-0.3	-0.3	0.2	0.3	1.0	0.8	0.0	0.0
A_9	-0.7	0.6	0.5	0.2	0.5	0.5	-0.5	0.5	-0.3	0.4	0.3	-0.5	0.5	-0.5	0.1	0.0	0.0	-0.2	-0.1	-0.2	0.1	0.0	0.1	-0.2	-0.2	0.3	1.0	0.3	0.4	-0.2	0.1
Br_8	0.0	0.0	0.2	0.9	0.3	0.9	-0.8	0.8	-0.5	0.5	0.5	-0.7	0.7	-0.9	0.0	0.0	-0.1	-0.4	-0.3	-0.3	0.2	0.0	0.1	0.4	0.6	1.0	0.3	0.2	0.1	-0.1	0.2
E_8	0.1	-0.2	-0.6	0.8	-0.5	0.3	-0.3	0.2	-0.1	0.1	0.1	0.1	-0.1	-0.3	-0.2	0.0	-0.1	-0.1	-0.1	-0.1	0.1	0.0	0.1	1.0	1.0	0.6	-0.2	-0.3	-0.3	0.2	0.0
A_8	0.2	-0.2	-0.8	0.6	-0.7	0.1	-0.2	0.1	0.0	0.0	0.0	0.3	-0.3	-0.1	-0.2	0.0	-0.1	0.0	0.0	0.0	0.1	-0.1	0.1	1.0	1.0	0.4	-0.2	-0.3	-0.3	0.3	-0.1
Br_7	0.0	0.0	0.0	0.1	0.0	0.2	-0.2	0.3	-0.1	0.2	0.1	-0.1	0.1	-0.2	-0.6	-0.8	-0.7	-0.1	0.0	0.0	0.8	-0.7	1.0	0.1	0.1	0.1	0.1	0.1	0.0	0.0	0.0
E_7	0.0	0.0	0.0	0.0	0.0	-0.1	0.1	-0.2	0.3	-0.2	-0.3	0.0	0.0	0.1	0.6	0.7	0.6	0.3	0.2	0.3	-0.7	1.0	-0.7	-0.1	0.0	0.0	0.0	0.0	0.0	0.0	0.0
A_7	0.0	0.0	0.0	0.1	0.0	0.2	-0.3	0.4	-0.3	0.3	0.3	-0.1	0.1	-0.2	-0.7	-0.8	-0.9	-0.2	-0.2	-0.2	1.0	-0.7	0.8	0.1	0.1	0.2	0.1	0.1	0.1	-0.1	0.1
Br_6	0.0	-0.1	-0.2	-0.3	-0.2	-0.3	0.3	-0.3	0.9	-0.6	-0.9	0.3	-0.3	0.4	0.3	0.2	0.3	1.0	1.0	1.0	-0.2	0.3	0.0	0.0	-0.1	-0.3	-0.2	-0.2	-0.2	-0.1	0.1
E_6	0.0	0.0	-0.2	-0.2	-0.2	-0.3	0.3	-0.3	0.9	-0.4	-0.9	0.3	-0.3	0.3	0.2	0.2	0.3	1.0	1.0	1.0	-0.2	0.2	0.0	0.0	-0.1	-0.3	-0.1	-0.2	-0.1	-0.1	0.1
A_6	0.0	-0.1	-0.3	-0.3	-0.3	-0.4	0.4	-0.4	1.0	-0.6	-1.0	0.4	-0.4	0.5	0.3	0.3	0.3	1.0	1.0	1.0	-0.2	0.3	-0.1	0.0	-0.1	-0.4	-0.2	-0.3	-0.2	-0.1	0.2
Br_5	0.0	0.1	-0.1	0.1	-0.2	0.3	-0.4	0.3	-0.3	-0.3	0.0	0.0	0.1	0.9	0.7	1.0	0.3	0.3	0.3	-0.9	0.6	-0.7	-0.1	-0.1	-0.1	0.0	0.0	0.0	0.0	0.0	0.0
E_5	0.0	0.0	0.0	0.0	0.0	0.0	-0.1	0.3	-0.3	-0.3	0.0	0.0	0.0	0.5	1.0	0.7	0.3	0.2	0.2	-0.8	0.7	-0.8	0.0	0.0	0.0	0.0	0.0	0.0	0.0	0.0	0.0
A_5	-0.1	0.1	0.3	0.0	0.3	0.0	0.2	-0.3	0.2	-0.1	-0.2	-0.2	0.3	0.0	1.0	0.5	0.9	0.3	0.2	0.3	-0.7	0.6	-0.6	-0.2	-0.2	0.0	0.1	0.1	0.1	-0.2	0.3
Br_4	0.2	-0.2	-0.4	-0.7	-0.5	-1.0	1.0	-0.9	0.6	-0.6	-0.6	0.8	-0.8	1.0	0.0	0.0	0.1	0.5	0.3	0.4	-0.2	0.1	-0.2	-0.1	-0.3	-0.9	-0.5	-0.5	-0.4	0.1	-0.1
E_4	-0.2	0.2	0.8	0.5	0.9	0.8	-0.7	0.8	-0.6	0.6	0.6	-1.0	1.0	-0.8	0.3	0.0	0.0	-0.4	-0.3	-0.3	0.1	0.0	0.1	-0.3	-0.1	0.7	0.5	0.6	0.5	-0.2	0.2
A_4	0.2	-0.2	-0.8	0.5	-0.9	-0.9	0.7	-0.8	0.6	-0.6	-0.6	1.0	-1.0	0.8	-0.2	0.0	0.0	0.4	0.3	0.3	-0.1	0.0	-0.1	0.3	0.1	-0.7	-0.5	-0.6	-0.5	0.2	-0.2
Br_3	-0.1	0.1	0.4	0.4	0.4	0.6	-0.5	0.5	-1.0	0.8	1.0	-0.6	0.6	-0.6	-0.2	-0.3	-0.3	-1.0	-0.9	-0.9	0.3	-0.3	0.1	0.0	0.1	0.5	0.3	0.4	0.3	0.1	-0.2
E_3	-0.2	0.2	0.4	0.4	0.4	0.6	-0.5	0.6	-0.7	1.0	0.8	-0.6	0.6	-0.6	-0.1	-0.3	-0.3	-0.6	-0.4	-0.6	0.3	-0.2	0.2	0.0	0.1	0.5	0.4	0.4	0.3	0.0	-0.2
A_3	0.1	-0.1	-0.4	-0.4	-0.4	-0.6	0.5	-0.5	1.0	-0.7	-1.0	0.6	-0.6	0.6	0.2	0.3	0.3	1.0	0.9	0.9	-0.3	0.3	-0.1	0.0	-0.1	-0.5	-0.3	-0.4	-0.3	-0.1	0.2
Br_2	-0.2	0.2	0.5	0.6	0.5	1.0	-1.0	1.0	-0.5	0.6	0.5	-0.8	0.8	-0.9	-0.3	-0.1	-0.4	-0.4	-0.3	-0.3	0.4	-0.2	0.3	0.1	0.2	0.8	0.5	0.5	0.4	-0.1	0.1
E_2	0.2	-0.2	-0.4	-0.7	-0.4	-1.0	1.0	-1.0	0.5	-0.5	-0.5	0.7	-0.7	1.0	0.2	0.0	0.3	0.4	0.3	0.3	-0.3	0.1	-0.2	-0.2	-0.3	-0.8	-0.5	-0.5	-0.4	0.1	-0.1
A_2	-0.2	0.2	0.5	0.7	0.6	1.0	-1.0	1.0	-0.6	0.6	0.6	-0.9	0.8	-1.0	0.0	0.0	-0.2	-0.4	-0.3	-0.3	0.2	-0.1	0.2	0.1	0.3	0.9	0.5	0.5	0.4	-0.2	0.2
Br_1	-0.2	0.2	1.0	0.1	1.0	0.6	-0.4	0.5	-0.4	0.4	0.4	-0.9	0.9	-0.5	0.3	0.0	0.1	-0.3	-0.2	-0.2	0.0	0.0	0.0	-0.7	-0.5	0.3	0.5	0.5	0.5	-0.3	0.2
E_1	0.0	0.0	-0.1	1.0	0.1	0.7	-0.7	0.6	-0.4	0.4	0.4	-0.5	0.5	-0.7	0.0	0.0	-0.1	-0.3	-0.2	-0.3	0.1	0.0	0.1	0.6	0.8	0.9	0.2	0.1	0.1	0.1	0.0
A_1	-0.2	0.2	1.0	-0.1	1.0	0.5	-0.4	0.5	-0.4	0.4	0.4	-0.8	0.8	-0.4	0.3	0.0	0.1	-0.3	-0.2	-0.2	0.0	0.0	0.0	-0.8	-0.6	0.2	0.5	0.6	0.5	-0.3	0.2
tau	-1.0	1.0	0.2	0.0	0.2	0.2	-0.2	0.2	-0.1	0.2	0.1	-0.2	0.2	-0.2	0.1	0.0	0.0	-0.1	0.0	-0.1	0.0	0.0	0.0	-0.2	-0.2	0.0	0.6	0.2	0.7	-0.1	0.1
rho	1.0	-1.0	-0.2	0.0	-0.2	-0.2	0.2	-0.2	0.1	-0.2	-0.1	0.2	-0.2	0.2	-0.1	0.0	0.0	0.0	0.0	0.0	0.0	0.0	0.0	0.2	0.1	0.0	0.0	-0.7	-0.1	-0.6	0.2

Table S2. Parameter correlation matrix for the best fit.

The correlation between the different parameters ranges from null (0) to total (1 or -1). Although some parameters are strongly correlated, the average correlation is relatively low, as shown by the average of the absolute values of the correlation parameters that is only 0.33.

It is especially important to remark the very low correlation of the thicknesses (of the dense Bi layer - t_{Bi} - and the nanostructured roughness layer - t_{rough}) with the Lorentz (A_i, E_i, Br_i) and Drude (rho, tau) parameters. This points at a very low correlation between the total nominal thickness of the Bi film and the dielectric function ε, thus underlining the reliability of our ellipsometry measurements and analysis for the accurate determination of both the total nominal thickness and ε from the far IR to the UV. This accuracy is confirmed by the independent RBS measurements (see **Results section** of the paper), which yield a value of the total nominal thickness of the Bi film very similar to that obtained by ellipsometry.

The correlation between t_{Bi} and t_{rough} is significant. However, these two parameters have been effectively decorrelated by performing the fits in restricted spectral ranges: (i) in the visible – UV the film is totally opaque and can be represented as a semi-infinite medium (Bi layer/roughness, with $t_{Bi} \rightarrow \infty$), thus t_{rough} can be determined independently; (ii) in the IR the film is partially transparent and thus a more realistic (substrate/Bi layer/roughness) model has to be used, in which both t_{Bi} and t_{rough} affect the ellipsometry spectra. Therefore, prior to performing the ellipsometry analysis in the full far IR – to – UV spectral range, we first fitted the visible – UV data using a Bi layer/roughness model with $t_{Bi} \rightarrow \infty$, to determine t_{rough}. Then we fitted the IR data with a substrate/Bi layer/roughness model in which t_{rough} was fixed at the previously determined value and t_{Bi} was a free parameter with a starting value equal to the thickness determined by RBS. This allowed to determine t_{Bi}. Finally we fitted the ellipsometry spectra in the full far IR – to – UV spectral range with the substrate/Bi layer/roughness model described in the paper. During this final step, both t_{Bi} and t_{rough} were free parameters, with their previously determined values being used as starting values for the fit. The best fit values of t_{Bi} and t_{rough} remained very similar to these starting values.

There is also a significant correlation between several parameters of the Lorentz oscillators: it means that there are several combinations of these oscillators that yield a similar ε spectrum in the full far IR – to – UV spectral range. Discussing in detail the correlation between these parameters is beyond the scope of this work, because at this point we do not aim at an accurate identification of the different optical transitions contributing to the obtained ε. Finally, it can be observed that the Drude parameters are very weakly correlated with those of the Lorentz oscillators, except oscillator nº9. This oscillator peaks at a low photon energy (0.12 eV) and is needed in the fit to account for a slight deviation of ε from a pure Drude behaviour in the far IR region of our measurement. This deviation remains to be ascertained and discussed. However, note that Tediosi et al. (ref. 11 of the paper) in their work had to use an "extended" Drude model to fit accurately their data in the far IR.

S2. Analysis of Thicker Films

Samples consisting of thicker Bi films on Si substrates were also grown and analysed. They show a very similar structure compared with the film studied in the **Results section** of the paper (this film with thickness $t_{bismuth\ nominal\ -\ RBS} = 78$ nm is denoted here as "78 nm film"). They consists of a dense Bi layer with a thin nanostructured Bi surface roughness layer on top.

Figure S2.1. (a) shows the experimental ellipsometric spectra of a sample consisting of a Bi film with $t_{bismuth\ nominal\ -\ RBS} = 141 \pm 4.5$ nm (denoted hereafter as "141 nm film") deposited on a Si substrate, together with the corresponding best fit spectra.
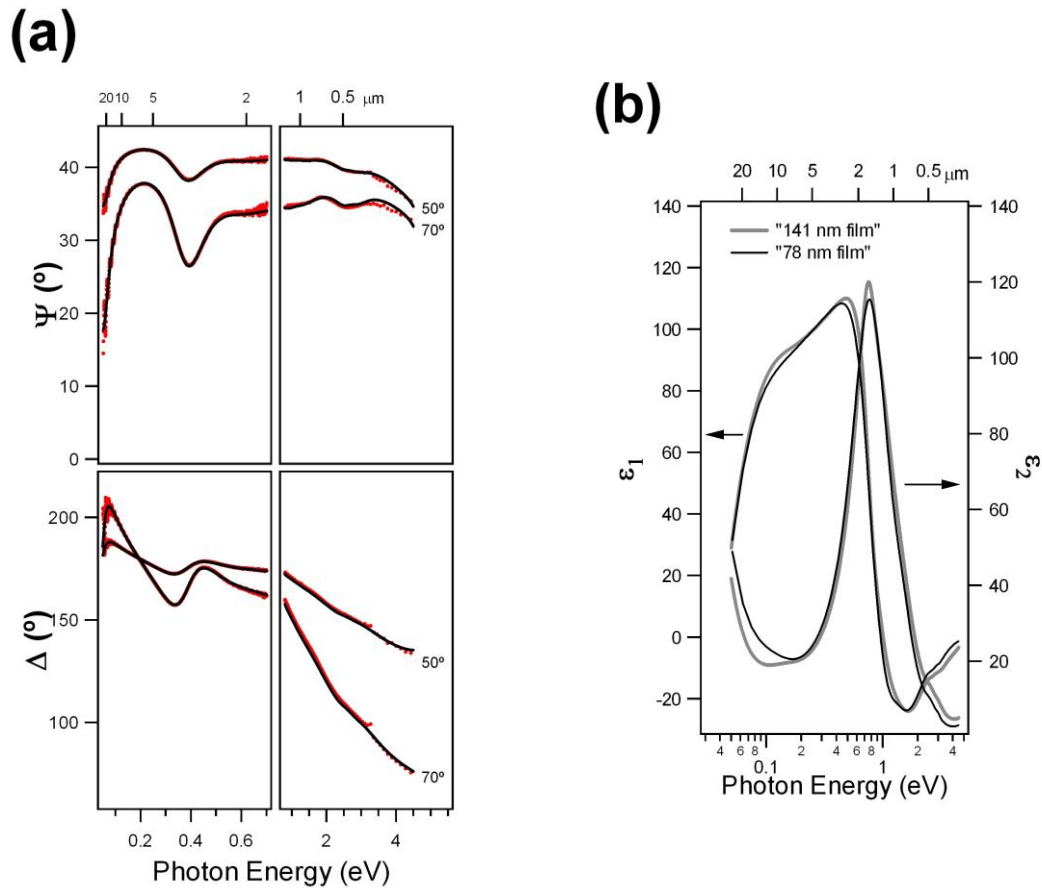
Figure S2.1. (a) Experimental (red dots) ellipsometric spectra (Ψ and Δ) and the corresponding best fit spectra (black curves) of a Bi film with $t_{nominal,\ RBS} = 141$ nm deposited on a Si substrate. (b) Best fit dielectric function $\varepsilon = \varepsilon_1 + j\varepsilon_2$ of the dense Bi layer in this film ("141 nm film") together with that of a thinner film ("78 nm film") taken from figure 3.

The spectra measured with the near IR to near UV and the IR setups show excellent spectral continuity, and the best fit spectra are in excellent agreement with the experimental ones. The best fit thicknesses for the dense Bi and nanostructured

6

roughness layers are $t_{bismuth} = 143$ nm and $t_{roughness} = 7$ nm. From these values, we obtain $t_{bismuth\ nominal\ -\ ellipsometry} = t_{bismuth} + 50\%\ t_{roughness} = 146.5$ nm, i.e. in very good agreement with the thickness obtained by RBS ($t_{bismuth\ nominal\ -\ RBS} = 141\pm\ 4.5$ nm). It is worth mentioning that both the Ψ and Δ spectra show an interferencial structure between 0.3 and 0.4 eV. This behaviour can be paralleled with the IR Mie-like resonances predicted for Bi nanospheres in the **Discussion and Applications section** of the paper. Let us remark that these photon energies correspond to wavelengths in vacuum between 3 μm and 4 μm, i.e. between 20 and 30 times longer than the film thickness. This points to a very high refractive index for the Bi dense layer in the $0.3 - 0.4$ eV region, i.e. very high ε_1 values. This is confirmed in figure S2.1. (b) that shows the best fit dielectric function ε of the dense Bi layer in the "141 nm film" together with that obtained for the "78 nm film". The obtained ε for both films are very similar showing the invariance of the dielectric function of Bi as a function of thickness. This also means that ε does not include any artifact due to correlation between the oscillator parameters and the thickness, thus further proving the consistency of our analysis.

S3. Crystalline Orientation of the Bismuth Films

The crystalline orientation of the Bi material grown on the Si substrate was studied by x-ray diffraction of the Cu Kα radiation, using a Philips X'PERT MPD diffractometer in the θ-2θ configuration. The obtained diffraction pattern obtained for the "78 nm film" is shown on figure S3.1.
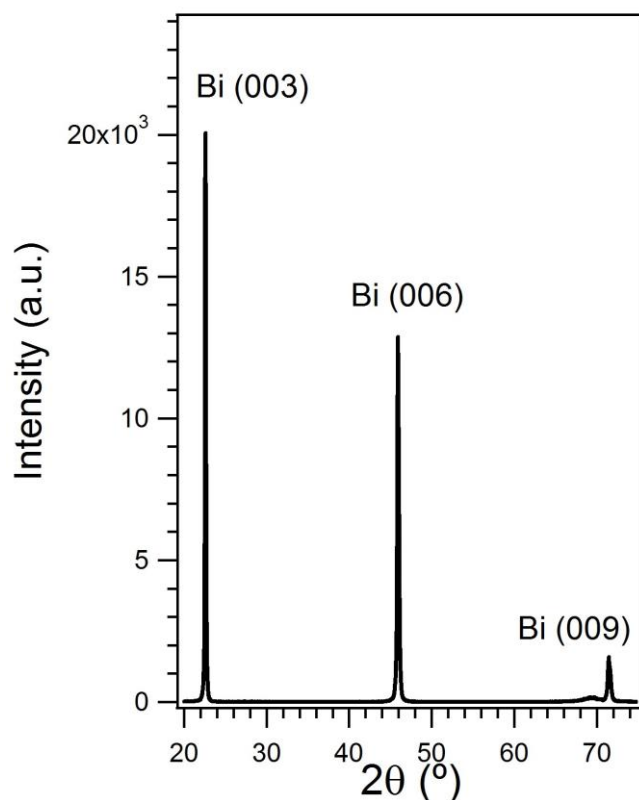

Figure S3.1. X-ray diffraction (θ-2θ) pattern of the "78 nm film"

The diffraction pattern is dominated by three peaks located at 22.6º, 45.9º, 71.5º. They result from diffraction by the Bi material, i.e. from Bi (003), Bi (006), Bi (009) respectively. This indicates a specific orientation of the Bi material, with its trigonal axis perpendicular to the substrate.[1] The weak diffraction structure around 69.4º results likely from diffraction by the Si substrate.

1 Kokorian, J.; Engelen, J.B.C.; de Vries, J.; Nazeer, H.; Woldering, L.A.; Abelmann, L.; *Ultra-flat bismuth films for diamagnetic levitation by template stripping*, Thin Solid Films **2014**, 550, 298.

S4. Mie Simulations of the Extinction Efficiency of Bismuth Nanospheres in a Non-vacuum Environment

We show here the optical extinction efficiency (Q_{ext}) spectra calculated with the Mie theory for a Bi nanosphere embedded in a transparent surrounding medium with a dielectric constant $\varepsilon_m = 4$. This value is typical of usual solid transparent embedding matrices. The dielectric function of Bi determined in this work (black lines in figure 3) was used for the nanosphere. Calculations were done for different nanosphere diameters D, from 100 nm to 2 μm. Figure S4.1. shows the obtained Q_{ext} spectra.
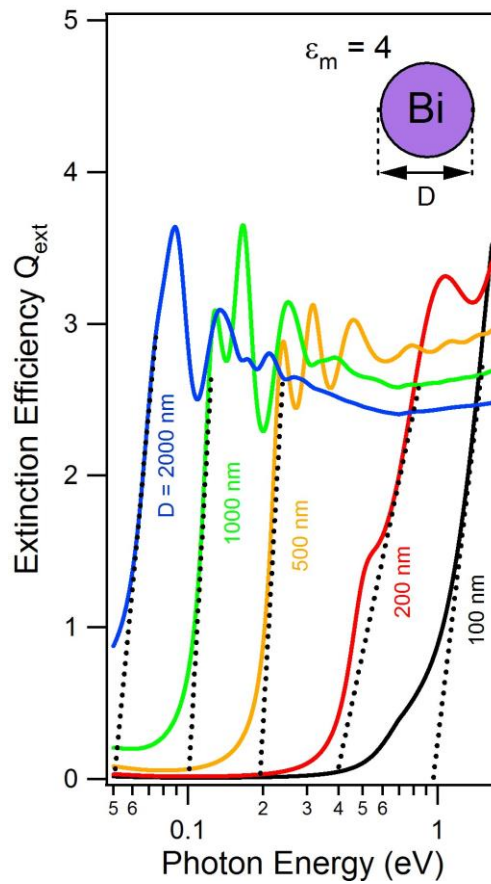

Figure S4.1. Extinction efficiency of a Bi nanosphere calculated using the Mie theory for different diameters D. The dielectric function of the nanosphere was that of Bi determined in our work (figure 3, thick black lines). The nanosphere is embedded in a transparent medium with a dielectric constant $\varepsilon_m = 4$.

The Q_{ext} spectra show a "bandgap-like" onset that shifts toward higher energies upon decreasing D. As indicated by the dotted lines, the corresponding "bandgap-like" value shifts from 0.05 eV to near 1 eV when D varies from 2 μm to 100 nm. In contrast with simulations done for the nanospheres in vacuum, no clear Mie-like resonance can be seen.

9

S5. Simulated Transmittance Spectra of Bismuth Films with Different Thicknesses

Figure S5.1 shows simulated transmittance spectra (at normal incidence) of Bi films on a SiO_2 substrate, for different film thicknesses t between 5 nm and 100 nm. The spectra have been calculated using the transfer matrix formalism, with the dielectric function of "bulk" Bi determined in our work (figure 3 of the paper, thick black lines). For a 100 nm thickness, the film is totally opaque in the visible – UV and partially transparent in the IR. Upon decreasing t, the strong absorption due to the interband transitions near 0.8 eV are clearly seen. These spectra provide a "bulk" reference to be compared with experimental data. Especially this would allow evaluating the role of electronic confinement in ultrathin films on the absorption band near 0.8 eV. To the best of our knowledge, neither the dependence of this absorption band on electronic confinement nor the far IR – to – UV optical response of ultrathin Bi films have been studied so far.
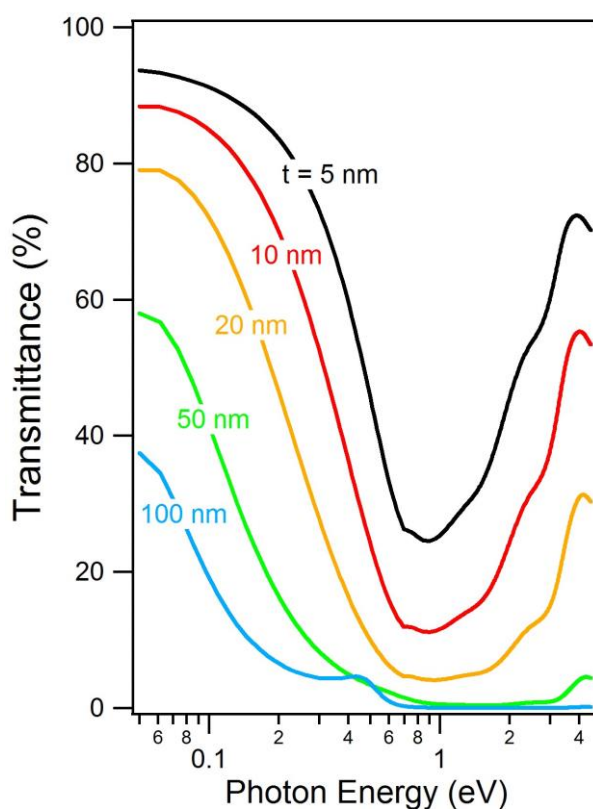

Figure S5.1. Simulated transmittance spectra (at normal incidence) of Bi films with different thicknesses t. The dielectric function of the films was that of Bi determined in our work (figure 3, thick black lines). The films stand on a SiO_2 substrate.